Journal of the American College of Cardiology Vol. 47, No. 10, 2006

Published by Elsevier Inc.
ISSN 0735-1097/06/$32.00
doi:10.1016/j.jacc.2005.12.063

Autologous Myoblast Transplantation for Chronic Ischemic Mitral Regurgitation

Emmanuel Messas, MD, MSc,*†‡§ Alain Bel, MD,*†‡§ Miguel Cortes Morichetti, MD,†‡§ Claire Carrion, PhD,‖ Marc D. Handschumacher, BS,¶ Séverine Peyrard, BS,# Jean Thomas Vilquin, PhD,‖ Michel Desnos, MD,*†‡§ Patrice Bruneval, MD,*§** Alain Carpentier, MD, PhD, FACC,*†‡§ Philippe Menasché, MD, PhD,*†‡§ Robert A. Levine, MD,¶ Albert A. Hagège, MD, PhD†‡§

Paris, France; and Boston, Massachusetts

OBJECTIVES This study was designed to assess whether post-myocardial infarction (MI) in-scar transplantation of skeletal myoblasts (SM) could reduce chronic ischemic mitral regurgitation (MR) by decreasing left ventricular (LV) remodeling.

BACKGROUND Extensive work has confirmed the relationship between ischemic MR and post-myocardial infarction (MI) remodeling of the LV.

METHODS An infero-posterior MI was created in 13 sheep, thereby resulting in increasing MR. Two months post-MI, the animals were randomized and in-scar injected with expanded autologous SM (n = 6, mean: 251 × 10^6 cells) or culture medium only (n = 7). Three-dimensional echocardiography was performed at baseline, before transplantation, and for two months thereafter (sacrifice), with measurements of LV end-diastolic and end-systolic volumes (ESV), ejection fraction (EF), MR stroke volume, and leaflet tethering distance; wall motion score index (WMSi) was assessed by two-dimensional echo.

RESULTS Measurements were similar between groups at baseline and before transplantation. At sacrifice, transplantation was found to have reduced MR progression (regurgitant volume change: −1.83 ± 0.32 ml vs. 5.9 ± 0.7 ml in control group, $p < 0.0001$) and tethering distance (−0.41 ± 0.09 cm vs. 0.44 ± 0.12 cm in control group, $p < 0.001$), with significant improvement of EF (2.01 ± 0.94% vs. −4.86 ± 2.23%, $p = 0.02$), WMSi (−0.25 ± 0.11 vs. 0.13 ± 0.03 in controls, $p < 0.01$) and a trend to a lesser increase in ESV (23.3 ± 3.5 ml vs. 35.4 ± 4.2 ml in control group, $p = 0.055$).

CONCLUSIONS Autologous skeletal myoblast transplantation attenuates mild-to-moderate chronic ischemic MR, which otherwise is progressive, by decreasing tethering distance and improving EF and wall motion score, thereby enhancing valve coaptation. These data shed additional light on the mechanism by which skeletal myoblast transplantation may be cardioprotective. (J Am Coll Cardiol 2006;47:2086–93) © 2006 by the American College of Cardiology Foundation

Ischemic mitral regurgitation (MR) is a common complication of ischemic heart disease that conveys an adverse prognosis after both myocardial infarction (MI) and coronary revascularization (1,2). Extensive work has confirmed the relation of ischemic MR to remodeling and distortion of the ischemic left ventricle (LV) (3–9). As viable myocardial cells are lost, the wall becomes thinner and bulges outward, a process that begins almost immediately and then progresses over weeks to months (10). If the inferior wall of the heart is involved, bulging of this wall also displaces the attached papillary muscles to which the mitral leaflets are anchored. Displacement of these muscles tethers the leaflets into the ventricular cavity and restricts their ability to close effectively at the level of the annulus, where they insert. This limits the surface over which the leaflets can make contact or coapt, resulting in MR (11–15).

Ischemic MR is therefore an imbalance of the entire mitral-ventricular complex, including the LV wall. Accordingly, reducing annular size alone, the standard therapeutic approach, is often ineffective because of persistent leaflet tethering to the displaced papillary muscles (PMs) and LV wall (16–18). We have shown that this process can be reversed by reshaping the heart surgically or with an external patch. However, with these approaches, sizeable noncontracting segments of the muscle wall remain, which do not contribute to output (8,19).

After isolation from a skeletal muscle biopsy, skeletal myoblasts (SMs) have the capability to proliferate in culture, to survive in ischemic fibrosis, and to fuse into myotubes, forming long-term viable grafts (20–24). In animals, after injection in a post-infarction scar, autologous SM transplantation (treatment) is effective to improve LV global and regional (within the infarcted area) function, to limit LV remodeling and decrease LV end-systolic volume (ESV) (25,26).

We therefore proposed the hypothesis that skeletal myoblast transplantation has the potential to reduce leaflet

From the *Université René Descartes Paris 5, Faculté de Médecine René Descartes Paris 5, Paris, France; †Institut National de la Santé et de la Récherche Médicale, Unité 633, Paris, France; ‡Ecole de Chirurgie, Paris, France; §Assistance Publique-Hôpitaux de Paris, Hôpital Européen Georges Pompidou, Paris, France; ‖INSERM U582, Institut de Myologie, Groupe Hospitalier Pitié-Salpêtrière, Paris, France; ¶Cardiac Ultrasound Laboratory, Massachusetts General Hospital, Harvard Medical School, Boston, Massachusetts; #Clinical Investigation Center 92010-INSERM, Paris, France; **Department of Pathology, INSERM U 430, Paris, France; and This study was supported by grants R21 HL 72353 (Drs. Messas, Menasché, Levine, and Hagège), R01 HL38176 (Drs. Messas, Carpentier, and Levine) and K24 67434 (Dr. Levine), National Institutes of Health, Bethesda, Maryland. Presented in part as an abstract in the Scientific Sessions of the American College of Cardiology, March 2004.

Manuscript received August 2, 2005; revised manuscript received November 1, 2005, accepted December 19, 2005.

Abbreviations and Acronyms

ESV = end-systolic volume
FBS = fetal bovine serum
IV = intravenously
LV = left ventricle
MHC = myosin heavy chain
MI = myocardial infarction
MR = mitral regurgitation
PM = papillary muscle
SM = skeletal myoblast
3D = three-dimensional
WMS = wall motion score

tethering distance and ischemic MR by locally reshaping the infarcted wall and improving global LV function (Fig. 1). This approach was tested in a chronic ischemic MR sheep model using three-dimensional (3D) and Doppler echocardiography to quantify MR and relate it to 3D changes in valve configuration.

METHODS

All experiments were performed in accordance with the "Guiding Principles in the Care and Use of Animals" of the American Physiological Society.

Chronic ischemic MR. We used the chronic ischemic MR model of Llaneras and Edmunds (27,28), which produces MR only with LV remodeling, eight weeks after ligating the second and third circumflex obtuse marginal coronary arteries. Thirteen sheep (40 to 50 kg), anesthetized with thiopentothal (0.5 ml/kg), intubated and ventilated at 15 ml/kg with 2% isofluorane and oxygen, and given glycopyrrolate (0.4 mg intravenously [IV]) and prophylactic vancomycin (0.5 g IV), underwent sterile left thoracotomy, with procainamide (15 mg/kg IV) and lidocaine (3 mg/kg IV followed by 2 mg/min) given 10 min before coronary ligation. Sheep received oral amiodarone (400 mg daily) for two days before infarction and oral acebutolol (200 mg) and aspirin (250 mg) the day before infarction. After baseline imaging, the pericardium was opened and the second and third circumflex obtuse marginal branches were ligated to infarct the infero-posterior wall. Imaging was repeated and the thoracotomy closed (Fig. 2A).

Cell transplantation. CELL CULTURES. At the time of infarction, a 10-mg skeletal muscle biopsy was obtained from the vastus lateralis. The biopsy was minced, frozen, and then cultured 14 days before transplantation (25). After enzymatic dissociation, the tissue was centrifuged and the remaining debris eliminated by filtration (100-μm mesh). Fourteen days before transplantation, the cells were plated onto Nunc substrates (10^3/cells/cm^2) and grown in Ham medium supplemented with fetal bovine serum (FBS) (20%, Perbio, Logan, Utah), beta-fibroblast growth factor (5 ng/ml, Sigma, St. Louis, Missouri) and penicillin-streptomycin (10,000 IU/ml and 10 mg/ml, respectively, Gibco, Invitrogen, Cergy Pontoise, France). Cells were expanded twice by trypsinization before reaching confluence, and the culture medium was then shifted to a differentiation medium containing no beta-fibroblast growth factor and 2% FBS.

PREPARATION OF CELLS. Fourteen days after plating, the cells were harvested by trypsinization for implantation.

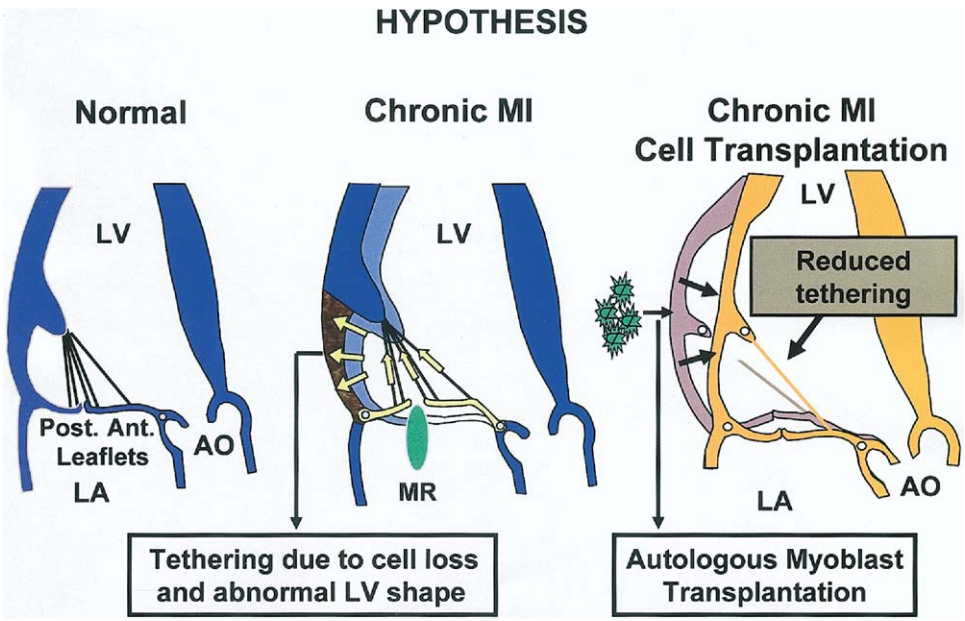

Figure 1. Mechanistic hypothesis of the efficacy of skeletal myoblast transplantation on chronic ischemic mitral regurgitation (MR). **(Left)** Baseline configuration of left ventricle (LV) with normal mitral leaflet closure. **(Middle)** Chronic infero-posterior infarction: loss of viable myocardial cells induce local LV remodeling with outward bulging of the free wall, papillary muscle displacement, and increased leaflet tethering and MR. **(Right)** Myoblast transplantation reverses local remodeling with decreased tethering distance and improved leaflet coaptation and MR. Ao = aorta; Ant. = anterior; LA = left atrium; MI = myocardial infarction; Post. = posterior.

JACC Vol. 47, No. 10, 2006
May 16, 2006:2086–93

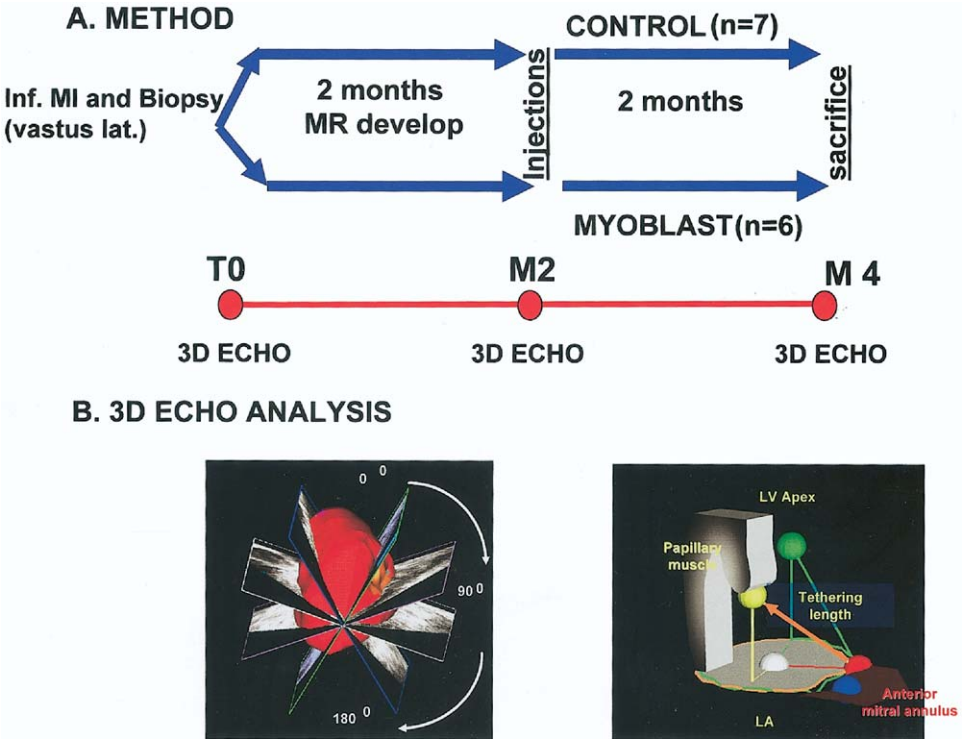

Figure 2. **(A)** Method. T0 = Infarction and vastus lateralis biopsy; M2 = two months after infarction: time for MR to develop and time of injections; M4 = four months after infarction: sacrifice. At each time point three-dimensional (3D) and two-dimensional echo analysis were performed. **(B)** 3D echo analysis. 3D left ventricular volumes were obtained using endocardial borders from nine views **(left)**. The least-squares plane of the mitral annular hinge points was established as reference frame; projecting the annulus onto this plane gave annular area. Mitral geometry was analyzed at mid-systole (time of closest leaflet-annulus approach), including papillary muscle-to-annulus tethering distance **(right)**. MI = myocardial infarction; MR = mitral regurgitation.

Following one rinse with Ca^{2+}- and Mg^{2+}-free phosphate-buffered saline (Gibco, Invitrogen), the cells were incubated for 5 min with trypsin-ethylene diamine tetra acetic. Upon dissociation, 10% (final volume) of FBS was added and the cells were centrifuged (1,200 rpm). The cell pellet was washed three times in saline (NaCl 0.9%, Baxter) supplemented with bovine serum albumin (0.5%, Sigma). Cell counting was performed using the Neubauer hemacytometer, and a first assessment of cell viability was done using the trypan blue dye exclusion technique. The cell pellet was then resuspended in saline to a final concentration of 10^8 cells/ml. Aliquots were preserved for further characterization of cell type and viability. Immediately before injection, cells were transferred to 1 ml syringes and warmed to room temperature.

INTRAMYOCARDIAL INJECTIONS. Sheep were randomized into two groups receiving culture medium only (n = 7, control group) or cells (n = 6, myoblast group) in a physiologic salt solution with 0.5% bovine serum albumin. Eight weeks after infarction, during a repeat left lateral thoracotomy, 20 to 30 intramyocardial myoblast injections were performed across the bulging infero-posterior infarcted area (mostly underlying the posterior papillary muscle) using a 27-gauge needle. Control sheep received an equivalent volume of culture medium.

Assessment of results. CELL CHARACTERIZATION. At each expansion time and at the final harvest, the cells were analyzed by flow cytofluorimetry for the CD56 myogenic marker. The proportion of myogenic cells was evaluated using flow immunofluorescence as previously described (26).

Ultrasonic assessment. ACQUISITIONS. After general anesthesia and during thoracotomy (for optimal imaging), examinations were performed: 1) at baseline; 2) immediately before injections (8 weeks after infarction, allowing MR to develop); and 3) 2 months after injections. Three-dimensional echo data were acquired with a 5-MHz epicardial transducer (Philips Sonos 5500), scanning through a water bath from the LV apex using a rotating array with its beam aligned through the center of the mitral valve, parallel to the LV long axis (29,30). Onboard 3D software recorded 30 rotated images automatically at 6° increments, with electrocardiographic gating and suspended respiration. Digital images were transferred to a Silicon Graphics workstation (Fig. 2B).

The 3D echo analysis first established a reference frame, the least-squares plane of the mitral annulus (29). Mitral geometry was analyzed within this reference frame from rotated images at mid-systole, the time of closest leaflet-annulus approach. The mitral and aortic annuli were identified as the leaflet hinge points, confirmed by cineloop review. The PMs were traced and their most basal and anterior tips identified by reviewing several adjacent images. The tethering length over which the leaflets and chordae were stretched between the PMs and the relatively fixed

Table 1. Echocardiographic Measurements

	Baseline		Chronic MI		Sacrifice	
	Control	Cell Transplantation	Control	Cell Transplantation	Control	Cell Transplantation
HR	99.5 ± 1.6	99.1 ± 2.7	103.1 ± 3.4	100.6 ± 3.6	109.7 ± 2.9	100.8 ± 4.9
EDV(ml)	32.01 ± 0.5	32.2 ± 1.6	63.4 ± 3.1*	62.6 ± 5.1*	111.0 ± 3.8†	102.3 ± 5.1†
ESV(ml)	10.5 ± 0.33	11.8 ± 0.5	39.1 ± 1.7*	39.7 ± 3.1*	75.4 ± 4.1†	63 ± 2.9†
EF	0.67 ± 0.01	0.63 ± 0.02	.38 ± 0.02*	.36 ± 0.02*	.33 ± 0.01	.38 ± 0.01
WMS indexed	0.0 ± 0.0	0.0 ± 0.0	1.25 ± 0.08*	1.19 ± 0.05*	1.39 ± 0.11†	.94 ± 0.13†
Tethering dist (cm)	2.48 ± 0.03	2.5 ± 0.05	3.07 ± 0.05*	2.9 ± 0.06*	3.5 ± 1.1†	2.51 ± 0.04†
MAA (cm^2)	5.8 ± 0.04	5.8 ± 0.19	6.8 ± 0.19*	6.3 ± 0.12*	7.2 ± 0.12†	6.6 ± 0.18†
MRSV (ml)	1.14 ± 0.2	1.33 ± 0.41	7.2 ± 0.59*	5.8 ± 0.59*	13.1 ± 0.77†	4 ± 0.51†
RF%	5.4 ± 0.9	6.3 ± 1.8	30 ± 0.5*	27.4 ± 4.8*	36 ± 1	10.5 ± 1.6†

All two-way ANOVAs but one (heart rate) were significant $p < 0.05$. Significant changes $p < 0.025$ (Bonferroni-corrected) are indicated for the two-way comparisons: *Baseline vs. chronic MI, †chronic MI vs. sacrifice.

EDV = left ventricular end-diastolic volume; EF = ejection fraction; ESV = left ventricular end-systolic volume; HR = heart rate; MAA = mitral annulus area; MI = myocardial infraction; MRSV = mitral regurgitation stroke volume; RF = regurgitation fraction; Tethering dist = three-dimensional tethering distance between posterior papillary tips and anterior mitral annulus; WMS = wall motion score.

fibrous portion of the annulus was then measured from posterior PM tip to the medial trigone of the aortic valve (medial junction of aortic and mitral annuli) (Fig. 2B, right). Tethering length was used because in previous studies it has emerged as the strongest predictor of ischemic MR (6–8,13). These 3D echo measurements have been shown to correlate well with those by sonomicrometer crystal array, both in vitro and in vivo ($r^2 = 0.99$, SEE = 0.7 mm, mean difference = 0.08 ± 0.7mm [NS vs. 0]) (6,8).

Two-dimensional epicardial echocardiography was performed for wall motion analysis scoring. One parasternal LV long-axis view was recorded, care being taken that the mitral and aortic valves and the apex were simultaneously visualized, with three parasternal short-axis views recorded at the base, PM, and apical levels. Acquisition of digital cineloops and analysis of segmental wall motion and MR stroke volume were performed by a single experienced operator blinded to the treatment group.

3D LV VOLUME, MITRAL GEOMETRY, AND MR EVALUATION. Three-dimensional LV volumes were obtained using endocardial border tracings from nine equally spaced rotated views (30). Mitral regurgitation stroke volume was calculated as LV stroke volume minus aortic outflow volume (measured by pulsed Doppler). Regurgitant fraction was calculated as (MR stroke volume)/(forward aortic + MR stroke volumes). Mitral annular area was calculated by projecting the mitral annular hinge points onto the least-squares reference plane. Mitral geometry was analyzed at mid-systole (time of closest leaflet-annulus approach), including the PM-to-annulus tethering distance previously described (6,8,13,15).

SCORING OF REGIONAL CONTRACTILITY. Using the three short-axis views, the LV was divided into 16 segments according to American Society of Echocardiography recommendations, and a score was allocated to each segment according to its contractility as (0) normokinetic, (+1) hypokinetic, (+2) akinetic, or (+3) dyskinetic. A global wall motion score (WMS) was derived from the algebraic sum of these values, and the WMS index was then obtained by dividing WMS by the total number of scored segments (n = 16) (31).

Pathologic assessment. Sacrifice was performed after the last ultrasonic evaluation, and the hearts were explanted and rinsed in a saline buffer. Location and extent of MI were visually assessed. The entire portion of the LV containing the MI was fixed in formalin for histology and immunohistochemistry.

HISTOLOGIC STUDIES. Formalin-fixed paraffin-embedded sections of the whole MI were stained with hematoxylin-eosin-safranin for qualitative assessment of scar and grafted cells focusing on fibrosis, fat tissue, inflammation, and myocyte necrosis; and presence, density, organization and differentiation of grafted cells.

IMMUNOHISTOCHEMICAL STUDIES. On selected paraffin sections, immunohistochemistry for skeletal fast isoform (MY-32 clone monoclonal antibodies (Sigma) and cardiac and skeletal slow isoforms (NOQ7 clone monoclonal antibodies (Sigma) of myosin heavy chain (MHC) was performed as previously described (25).

Statistical analysis. Echocardiographic measurements were compared among stages and sheep by repeated-measures ANOVA. Significant ANOVAs were explored by two paired *t* tests (chronic ischemia vs. baseline and vs. sacrifice), with significance at $p < 0.025$ (Bonferroni-corrected). Differences in progression between the two groups were explored by unpaired *t* test, with significance at $p < 0.05$. All data were reported as means ± SEM. Statistical analysis used StatView 5.0. Reproducibility of echographic measurements was tested by two independent observers and gave a variability of 2.5% of the mean.

RESULTS

Myocardial infarction was created in 13 animals: 7 controls and 6 given myoblasts. All animals remained available for echocardiography at two months after infarction (pretreatment) and at time of sacrifice (4 months post-MI). Param-

JACC Vol. 47, No. 10, 2006
May 16, 2006:2086–93

eters were similar between groups at baseline and at 2 months (pretreatment) (Table 1, columns 1 and 2).

Cell cultures. Cultures yielded to 251 ± 42 million cells (170 to 150 million) with 60 ± 2.7% (50% to 70%) myogenic cells.

3D ultrasonic functional assessment and evaluation of MR. PROGRESSION OF ISCHEMIC MR. At the time of acute infarction, LV dilation was limited and, as at baseline, the leaflets closed at the annular level with only trace MR. At two months post-MI, LV volume was comparable between groups (+30.4 ± 5.6 ml in treatment group vs. +31.4 ± 3.5 ml in control group for end-diastolic volume, $p = 0.32$; and +28.1 ± 5.9 ml in treatment group vs. +28.56 ± 2.09 ml in control group for end-systolic volume, $p = 0.31$). With bulging of the affected wall, the leaflets were apically tented with mild-to-moderate MR (regurgitant fraction: 27.4 ± 4.8% vs. 30 ± 5% in the treatment and control groups, respectively; $p = 0.51$). Papillary muscle tip displacement away from the annulus was comparable between groups (2.9 ± 0.06 cm vs. 3.07 ± 0.05 cm, $p = 0.87$) (Table 1, Fig. 3).

REVERSAL OF ISCHEMIC MR. Two months after myoblast treatment (i.e., 4 months post-infarction), there was a reduction in ischemic MR (5.8 ± 0.59 ml/beat before treatment vs. 4.0 ± 0.51 ml/beat 2 months after treatment, $p < 0.01$) and in MR progression (regurgitant volume: −1.83 ± 0.32 ml/beat vs. 5.9 ± 0.7 ml/beat in the treatment and control groups, respectively, $p < 0.0001$) (Figs. 3 and 4A), with a reduction of tethering distance (2.9 ± 0.06 cm pretreatment vs. 2.51 ± 0.04 cm 2 months after treatment in the treated group, $p < 0.01$) and in its progression (−0.41 ± 0.09 cm vs. 0.44 ± 0.12 cm in the treatment and control groups, respectively, $p < 0.001$) (Fig. 4B). This paralleled a significant improvement of the left ventricular ejection fraction (+2.01 ± 0.94% in treatment group vs. −4.86 ± 2.23% in control group, $p = 0.02$) (Fig. 5A) and WMS index (−0.25 ± 0.11 in treatment group vs. 0.13 ± 0.03 in control group, $p < 0.01$) (Fig. 5B). The benefits of myoblast treatment were also suggested by a trend (almost significant) to a lesser increase in global ESV (23.3 ± 3.5 ml in the treatment group vs. 35.4 ± 4.2 ml in control group, $p = 0.055$). Mitral annular area increased eight weeks post-MI in parallel with development of MR, but its progression did not decrease significantly after treatment (Table 1).

Pathologic assessment. Scar sizes were similar between the two groups and always extended to the posterolateral LV wall and the posteromedial papillary muscle. In control subjects, scars were always transmural, with fibrous tissue intermingled with fat tissue (Fig. 6A). In the majority (5 of 6) of transplanted animals, large areas of grafted cells were

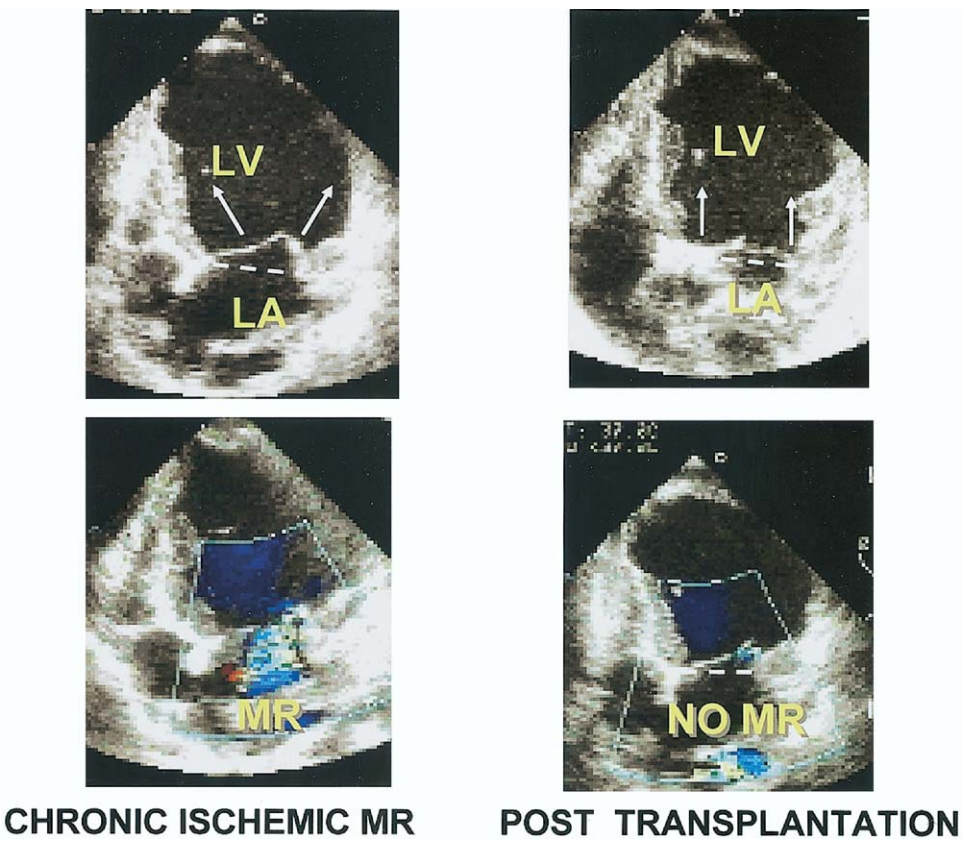

Figure 3. Mid-systolic apical two-dimensional echo images. **(Left)** Mild bulging of the infarcted infero-posterior wall with apical leaflet tenting relative to the annulus **(dashes)** in the direction of tethering **(upward arrows)**. Mild-to-moderate MR in the more globular remodeled LV is seen below. **(Right)** Cell transplantation restores a more normal LV shape with less bulging of the infero-posterior wall **(upward arrows)** and decreases tethering distance with improved coaptation and no MR **(bottom panel)** despite important LV dilation. Abbreviations as in Figure 1.

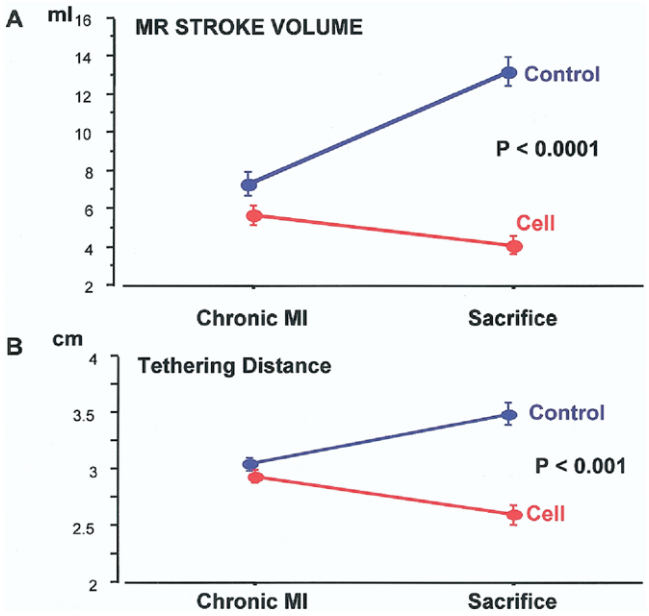

Figure 4. Efficacy of myoblast transplantation. Parallel variations in mitral regurgitation (MR) stroke volume **(A)** and tethering distance **(B)**. MI = myocardial infarction.

found within the scars (Fig. 6B). These cells displayed typical histologic features of well-differentiated skeletal myotubes (Fig. 7A) and often had a tendency to organize in parallel (Fig. 7B). In all transplanted animals, antibodies directed against the fast MHC isoform identified the presence of skeletal muscle structures surrounded by fibrotic and residual cardiac tissue, which was not labeled (Fig. 7C). Grafted myocytes maintained their skeletal myocyte differentiation and were all negative for the slow MHC isoform (Fig. 7D).

DISCUSSION

Ischemic MR is principally caused by LV remodeling with outward PM displacement and increased tethering (4–16). The current study assessed whether chronic ischemic MR can be reduced using autologous skeletal muscle transplantation within the infarcted area at a chronic stage (20–23).

Skeletal myoblasts are precursor cells located under the basal lamina of the adult skeletal muscle and committed to multiply after injury (32). They possess a high potential for division in culture and further multiplication after intramyocardial grafting (33).

Our hypothesis was that myoblast transplantation can reduce ischemic MR through a decrease in localized LV wall deformation and bulging. In the chronic post-MI setting, such a procedure has been effective experimentally in improving global and regional LV systolic function and limiting LV remodeling (25,26). In the current study, myoblast transplantation successfully decreased chronic mild-to-moderate ischemic MR (that was otherwise progressive) by significantly decreasing leaflet tethering distance, consistent with infarct zone reshaping, and repositioning the PM closer to the annulus. This can be understood based on the known dependence of ischemic MR on *localized* LV remodeling and the central and predominant role of tethering as the final common pathway in inducing ischemic MR, independent of global LV size and function (6,10,11,13). The decrease in tethering length is consistent with the engraftment of myotubes within the infarcted wall and the potential cell-mediated changes in extracellular matrix (34). This mechanistic hypothesis actually fits with previous experiments in which small displacements of the PM tip created large, nonlinear changes in MR (6,8,9). The mild reduction in abnormal wall motion score may reflect limitation of remodeling and outward infarct bulging by new cell growth. This limitation of LV remodeling could explain the significantly lower EF deterioration in the cell group, and the lower ESV increases (25,26). It is beyond the scope of this study to determine whether myoblast transplantation may also provide benefits other than limitation of remodeling, which might include contraction of engrafted myotubes fused with host cardiomyocytes or paracrine mobilization of cardiac stem cells (35,36).

Study limitations and future directions. The scope of this study is sharply focused on the problem of inferoposterior MI, a common cause of ischemic MR. In case of global LV dysfunction, the major determinant of MR remains the displacement of the PMs, which are located in the posterior portion of the LV. Therefore, a similar approach could in principle achieve a beneficial effect by injecting skeletal myoblasts around both PM regions (6). Finally, these positive results could justify further studies using percutaneous techniques of myoblast delivery, particularly through the coronary veins (37).

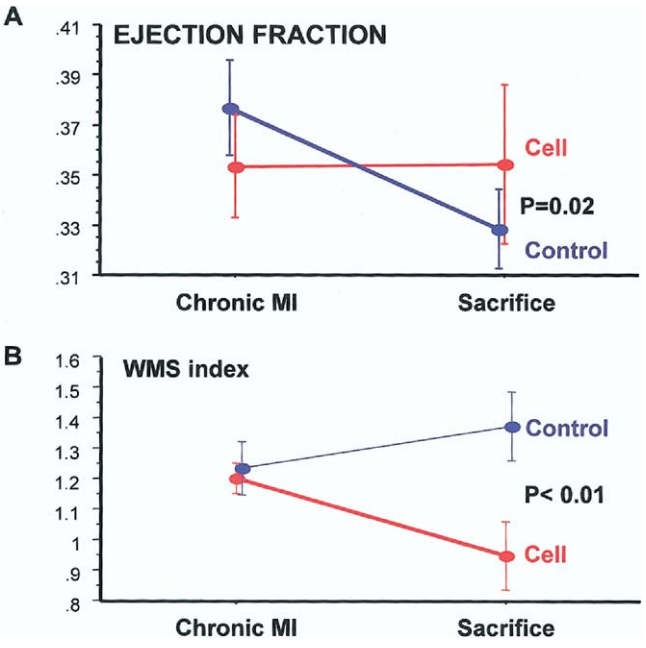

Figure 5. Effects of myoblast transplantation on left ventricular ejection fraction function **(A)** and wall motion score (WMS) **(B)**. MI = myocardial infarction.

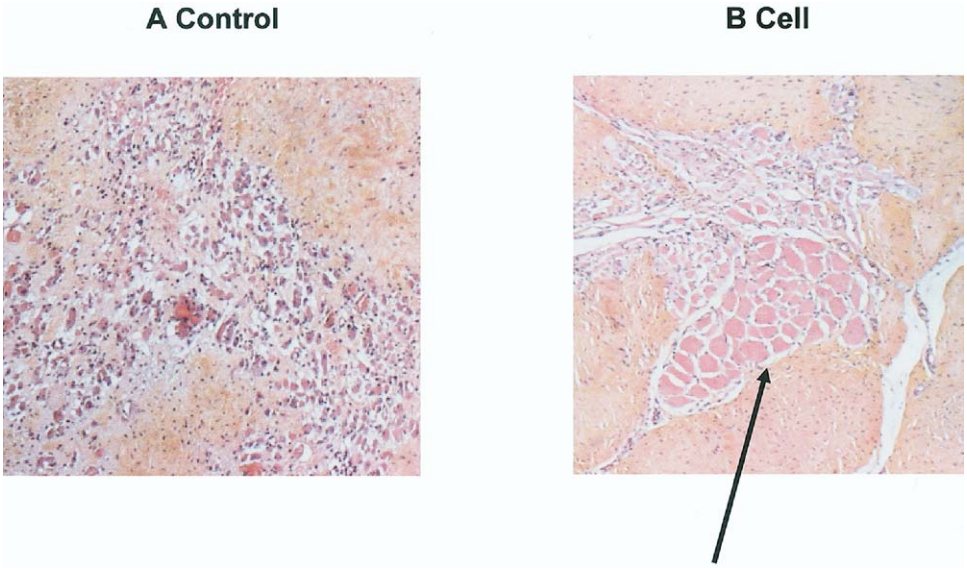

Figure 6. Histology of the subpapillary muscle region. **(A)** Chronic infarction (after four months) in a control animal characterized by dense fibrous tissue (H&E stain, **bar** = 600 μm). **(B)** Scar area in a grafted sheep at two months after transplantation with identification of a group of well-differentiated grafted cells **(black arrow)** replacing fat and fibrous tissues (H&E stain, **bar** = 600 μm).

Conclusions. In the chronic post-infarction setting, autologous skeletal myoblast transplantation attenuates mild-to-moderate chronic ischemic MR, which is otherwise progressive, by decreasing tethering distance over which the leaflets are stretched and improving ejection fraction and wall motion score, thereby enhancing valve coaptation. Given the limitations of existing methods for repairing ischemic MR in patients (38), it is conceivable that such a procedure may be considered as a complement to standard surgical therapy in the future.

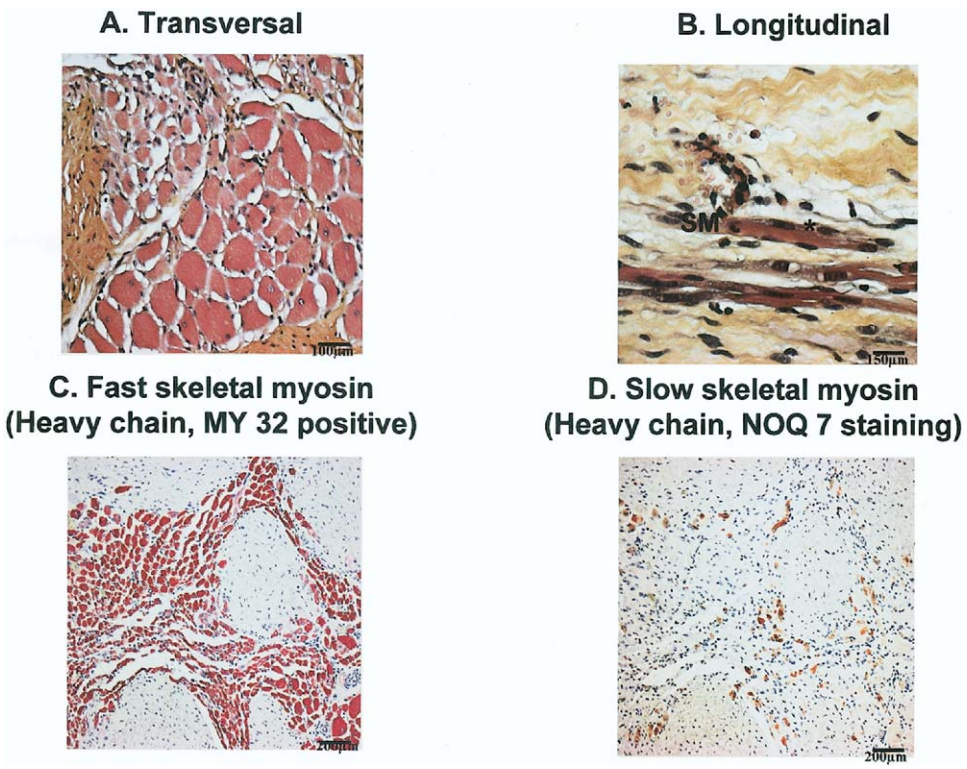

Figure 7. Organized skeletal muscle cells. Treated area in a grafted sheep at two months after transplantation. **(A)** (×40) High density of grafted cells on traversal section and surrounded by fibrous tissue (H&E stain; **bar** = 100 μm). **(B)** (×300) Skeletal myotubes (SM) organized in parallel with multiple peripheral nuclei **(*)** and abundant myofilaments (H&E stain; **bar** = 150 μm). **(C)** Section of an engrafted scar area at two months after transplantation. Immunostaining for the fast isoform of the beta myosin heavy chain (My 32; **bar** = 200 μm). **(D)** To a serial section, immunostaining for the slow isoform of beta myosin heavy chain (NOQ7; **bar** = 200 μm).

Reprint requests and correspondence: Dr. Emmanuel Messas, Cardiology Department, Hôpital Européen Georges Pompidou, INSERM U 633, Hôpital Broussais, 6 rue Didot, 75014 Paris, France. E-mail: emmanuel.messas@nck.aphp.fr.

REFERENCES

1. Lamas GA, Mitchell GF, Flaker M, et al., for the Survival and Ventricular Enlargement Investigators. Clinical significance of mitral regurgitation after acute myocardial infarction. Circulation 1997;96: 827–33.
2. Grigioni F, Enriquez-Sarano M, Zehr KJ, Bailey KR, Tajik AJ. Ischemic mitral regurgitation: long-term outcome and prognostic implications with quantitative Doppler assessment. Circulation 2001; 103:1759–64.
3. Rumberger JA. Ventricular dilatation and remodeling after myocardial infarction. Mayo Clin Proc 1994;69:664–74.
4. Godley RW, Wann LS, Rogers EW, Feigenbaum H, Weyman AE. Incomplete mitral leaflet closure in patients with papillary muscle dysfunction. Circulation 1981;63:565–71.
5. Kono T, Sabbah HN, Rosman H, et al. Mechanism of functional mitral regurgitation during acute myocardial ischemia. J Am Coll Cardiol 1992;19:1101–5.
6. Otsuji Y, Handschumacher MD, Schwammenthal E, et al. Insights from three-dimensional echocardiography into the mechanism of functional mitral regurgitation: direct in vivo demonstration of altered leaflet tethering geometry. Circulation 1997;96:1999–2008.
7. He S, Fontaine A, Ellis JT, Schwammenthal E, Yoganathan AP, Levine RA. An integrated mechanism for functional mitral regurgitation: leaflet restriction vs. coapting force—in vitro studies. Circulation 1997;96:1826–34.
8. Liel-Cohen N, Guerrero JL, Otsuji Y, et al. Design of a new surgical approach for ventricular remodeling to relieve ischemic mitral regurgitation: insights from three-dimensional echocardiography. Circulation 2000;101:2756–63.
9. Messas E, Guerrero JL, Handschumacher MD, et al. Paradoxic decrease in ischemic mitral regurgitation with papillary muscle dysfunction: insights from three-dimensional and contrast echocardiography with strain rate measurement. Circulation 2001;104:1952–7.
10. Sabbah HN, Kono T, Stein PD, Mancini GBJ, Goldstein S. Left ventricular shape changes during the course of evolving heart failure. Am J Physiol 1992;263:H266–70.
11. Sabbah HN, Kono T, Rosman H, Jafri S, Stein PD, Goldstein S. Left ventricular shape: a factor in the etiology of functional mitral regurgitation in heart failure. Am Heart J 1992;123:961–6.
12. Agricola E, Oppizzi M, Maisano F, et al. Echocardiographic classification of chronic ischemic mitral regurgitation caused by restricted motion according to tethering pattern. Eur J Echocardiogr 2004;5: 326–34.
13. Otsuji Y, Handschumacher MD, Liel-Cohen N, et al. Mechanism of ischemic mitral regurgitation with segmental left ventricular dysfunction: three-dimensional echocardiographic studies in models of acute and chronic progressive regurgitation. J Am Coll Cardiol 2001;37: 641–8.
14. Messas E, Guerrero JL, Handschumacher MD, et al. Chordal cutting: a new therapeutic approach for ischemic mitral regurgitation. Circulation 2001;104:1958–63.
15. Yiu SF, Enriquez-Sarano M, Tribouilloy C, Seward JB, Tajik AJ. Determinants of the degree of functional mitral regurgitation in patients with systolic left ventricular dysfunction: a quantitative clinical study. Circulation 2000;102:1400–6.
16. Hung J, Papakostas L, Tahta SA, et al. Mechanism of recurrent ischemic mitral regurgitation after annuloplasty: continued LV remodeling as a moving target. Circulation 2004;110:II85–90.
17. Wu AH, Aaronson KD, Bolling SF, Pagani FD, Welch K, Koelling TM. Impact of mitral valve annuloplasty on mortality risk in patients with mitral regurgitation and left ventricular systolic dysfunction. J Am Coll Cardiol 2005;45:381–7.
18. Tahta SA, Oury JH, Maxwell JM, Hiro SP, Duran CM. Outcome after mitral valve repair for functional ischemic mitral regurgitation. J Heart Valve Dis 2002;11:11–9.
19. Hung J, Guerrero JL, Handschumacher MD, Supple G, Sullivan S, Levine RA. Reverse ventricular remodeling reduces ischemic mitral regurgitation: echo-guided device application in the beating heart. Circulation 2002;106:2594–600.
20. Menasché P, Hagège AA, Scorsin M, et al. Myoblast transplantation for heart failure. Lancet 2001;357:279–80.
21. Chiu RCJ, Zibaitis A, Kao RL. Cellular cardiomyoplasty: myocardial regeneration with satellite cell implantation. Ann Thorac Surg 1995; 60:12–8.
22. Taylor DA, Atkins ZB, Hungspreugs P, et al. Regenerating functional myocardium: improved performance after skeletal myoblast transplantation. Nature Med 1998;4:929–33.
23. Atkins BZ, Hueman MT, Meuchel JM, Cottman MJ, Hutcheson KA, Taylor DA. Myogenic cell transplantation improves in vivo regional performance in infarcted rabbit myocardium. J Heart Lung Transplant 1999;18:1173–80.
24. Levin HR, Oz MC, Chen JM, Packer M, Rose EA, Burkhoff D. Reversal of chronic ventricular dilation in patients with end-stage cardiomyopathy by prolonged mechanical unloading. Circulation 1995;91:2717–20.
25. McConnell P, Del Rio C, Jacoby D, et al. Correlation of autologous skeletal myoblast survival with changes in left ventricular remodeling in dilated ischemic heart failure. J Thorac Cardiovasc Surg 2005;130: 101–9.
26. Ghostine S, Carrion C, Souza LC, et al. Long-term efficacy of myoblast transplantation on regional structure and function after myocardial infarction. Circulation 2002;106:II31–6.
27. Llaneras MR, Nance ML, Streicher JT, et al. Pathogenesis of ischemic mitral insufficiency. J Thorac Cardiovasc Surg 1993;105:439–43.
28. Llaneras MR, Nance ML, Streicher JT, et al. Large animal model of ischemic mitral regurgitation. Ann Thorac Surg 1994;57:432–9.
29. Levine RA, Handschumacher MD, Sanfilippo AJ, et al. Three-dimensional echocardiographic reconstruction of the mitral valve, with implications for the diagnosis of mitral valve prolapse. Circulation 1989;80:589–98.
30. Handschumacher MD, Lethor JP, Siu SC, et al. A new integrated system for three-dimensional echocardiographic reconstruction: development and validation for ventricular volume with application in human subjects. J Am Coll Cardiol 1993;21:743–53.
31. Schiller NB, Shah PM, Crawford M, et al. Recommendations for quantitation of the left ventricle by two-dimensional echocardiography. J Am Soc Echocardiogr 1989;2:358–67.
32. Murray CE, Wiseman RW, Schwartz SM, Hauschka SD. Skeletal myoblast transplantation for repair of myocardial necrosis. J Clin Invest 1996;98:2512–23.
33. Allen RE, Rankin LL. Regulation of satellite cells during skeletal muscle growth and development. Proc Soc Exp Biol Med 1990;194: 81–6.
34. Murtuza B, Suzuki K, Bou-Gharios G, et al. Transplantation of skeletal myoblasts secreting an IL-1 inhibitor modulates adverse remodeling in infarcted murine myocardium. Proc Natl Acad Sci USA 2004;101:4216–21.
35. Rubart M, Soonpaa MH, Nakajima H, Field LJ. Spontaneous and evoked intracellular calcium transients in donor-derived myocytes following intracardiac myoblast transplantation. J Clin Invest 2004; 114:775–83.
36. Al Attar N, Carrion C, Ghostine S, et al. Long-term (1 year) functional and histological results of autologous skeletal muscle cells transplantation in rat. Cardiovasc Res 2003;58:142–8.
37. Brasselet C, Morichetti M, Messas E, et al. Skeletal myoblast transplantation through a catheter-based coronary sinus approach: an effective means of improving function of infarcted myocardium. Eur Heart J 2005;26:1551–6.
38. Aklog L, Flores KQ, Chen RH, et al. Does coronary artery bypass grafting alone correct moderate ischemic mitral regurgitation? Circulation 2000;102:II487–92.